

RESEARCH

Open Access



Optimization and Characterization of Cementitious Composites Combining Maximum Amounts of Waste Glass Powder and Treated Glass Aggregates

Sarra Mezaouri^{1*} , Zine El-Abidine Kameche¹, Hocine Siad², Mohamed Lachemi², Mustafa Sahmaran³ and Youcef Houmadi⁴

Abstract

This work investigates the combined use of waste glass aggregates (GA) and glass powder (GP) in cementitious mortars. For this reason, the optimized incorporation of GA by natural aggregates (NA) replacements was first studied after applying a surface roughening method with hydrofluoric acid. The compressive strength results were utilized to select the best mixture with GA. Then, different GP contents were added by cements substitutions to the optimized GA-based mortar. A control mortar without GA and GP amounts was also casted as a reference for comparison. The detailed mechanical, physical and durability properties of the resulted mixtures with combined GA and GP were assessed by considering the compressive and flexural strengths, ultra-sonic pulse velocity, alkali-silica reaction (ASR), rapid chloride permeability test (RCPT), magnesium sulphate attack and sulfuric acid resistance. The microstructure of different optimized (GA + GP)-combinations was characterized by scanning electron microscopy (SEM) and energy dispersive X-ray spectroscopy (EDS) in order to analyse the interfacial transition zone (ITZ) between glass materials and the surrounding matrix. The results showed that the optimized composition with 75% GA and 25% GP was shown with high compacity and durability characteristics due to the increased GA/matrix ITZ and the formation of C-(N,K)-S-H products with C-S-H.

Keywords Glass aggregates, Glass powder, Chemical treatment, Sustainability, Durability

Journal information: ISSN 1976-0485 / eISSN 2234-1315.

*Correspondence:

Sarra Mezaouri

sarra.mezaouri@univ-temouchent.edu.dz; sarrati28mezaouri@gmail.com

¹ Smart Structures Laboratory (SSL), Department of Civil Engineering and Public Works, Aïn-Temouchent University, P. Box: 284, 4600 Aïn-Temouchent, Algeria

² Department of Civil Engineering, Toronto Metropolitan University, Toronto, ON, Canada

³ Department of Civil Engineering, Hacettepe University, Ankara, Turkey

⁴ Smart Structures Laboratory (SSL), Department of Civil Engineering, Aïn-Temouchent University, Tlemcen University, P. Box: 119, 13000 Tlemcen, Algeria

1 Introduction

Glass products such as bottles, windows, screens, etc., are among the highly produced materials nowadays with a global amount of around 130 million tons, from which more than 100 million of glass waste is being stockpiled or disposed every year (Anand, 2021). This accounts for a large portion of nearly 5% of the total solid wastes discarded in landfills according to the World Bank Group 2018. Its extremely long biodegradation time, which may take up to a 1 million year for regular glass bottles (Serati et al., 2022), can create a major ecological problem if appropriate environmentally friendly solutions are not considered in the future. Although most glass wastes (GW) can be recycled in new industrial processes, there

are still limitations regarding the required energy to remove impurities and to achieve a new glassy material with the same quality as the original product (Tamanna & Tuladhar, 2020). In addition, the landfilled glasses are generally blended with various colours and chemical compositions, which necessitate specialized sorting facilities that cannot be found in all countries and regions. Thus, only 10 to 30% of waste glass is currently being reused for the production of new materials, depending on the locally available recycling infrastructures and regulations around the world (Rivera et al., 2018). This caused a large excess of waste glass that requires to be valorized for other alternatives. For this reason, the incorporation of GW in construction applications is gaining importance from specialists as one of the most valuable technical, environmental and economical solution to reduce the disposed quantities (Idir, 2009).

Up to now, there have been many published results on the inclusion of GW in concrete and mortar compositions, particularly as powder or aggregates (Ho & Huynh, 2022; Manzoor et al., 2022; Omoding et al., 2021; Tahwia et al., 2022; Wei et al., 2020). Recent works confirmed that finely ground glass has pozzolanic properties and can be used successfully as a supplementary cementitious material (SCM) for the partial replacement of cement (Higuchi et al., 2021; Omran et al., 2018). Although some promising mechanical and durability properties were reported for concretes and mortars incorporating fine glass powder (GP), there have been inconsistent findings about the optimized amounts by cement substitution. For example, Shoaie et al., (2020) showed that the best mechanical strengths and transport properties of cementitious composites were reached with the use of fine glass particles of up to 30% contents. However, other researchers such as (Elaqra & Rustom, 2018a) revealed that the substitution of 20% of cement by GP caused increased compressive strengths of mortars, which dropped sharply at 25% and 30% contents. Also, Nahi et al., (2020) who studied the inclusion of different-size glass powders by cement and sand replacements, indicated that the compressive strength of mortars decreased with increased glass powder at 28-day curing time, regardless of the size of GP particles. Although most the available literature agreed about the alkali-silica reaction (ASR) risk related to recycled glass aggregates, there is also discrepancies about the optimum properties and contents of GW to be used as recycled aggregates in cementitious materials. Indeed, glass aggregates (GA) were generally proven to generate ASR problem (Bueno et al., 2020), as a result of the chemical reaction between their amorphous silica content and alkalis (Na^+ , K^+ and Ca^{2+}) in cementitious networks. ASR can first cause expansion due to the formation of a hygroscopic gel with the property to

absorb water and enlarge, then cracks might develop and deteriorate the in-service performance of cementitious composites, especially under high relative humidity conditions of $\geq 70\%$ (Chihaoui et al., 2022). Some studies have linked this expansion directly to the size of aggregates and suggested glass particle sizes of lower than 600 μm to safely incorporate them as sand in mortars and concretes (Guo et al., 2020; Rajabipour et al., 2010). Nevertheless, Idir et al. (2010) found that a size of around 0.9–1 mm was the threshold to avoid ASR in mortars. Also, Lee et al. (2011) indicated a maximum size of 1.18 mm to avoid the deleterious expansion effect of GA. Apart from the particle size, the chemical composition, colour and origin of glass were also shown to induce different effects on ASR reaction level (Hwee & Du, 2013; Gorospe et al., 2019; Liu et al., 2015; Mohajerani et al., 2017; Saha et al., 2018; Saccani et al., 2017; Shayan et al., 2004; Saccani et al., 2010). This was maybe the reason for the inconsistent findings over the maximum amount of GW that can replace normal aggregates without raising the ASR concerns in cementitious materials, though the general trend of results established a higher ASR expansion at increased contents of recycled GA (Mohajerani et al., 2017; Tan & Du et al., 2013a). In line with these explanations, various glass aggregate contents, such as 20% found by Ismail and AL-Hashmi (2009), 30% by Romero and James (2013), 50% by Penacho and Brito (2014) and 100% by Sikora and Horszczaruk (2017), were presented as the optimum for reaching equal/greater mechanical strengths than the control mixtures.

In attempts to limit the ASR-related expansion of mortars and concretes containing recycled glass aggregates, several researches have tested the use of SCMs such as fly ash, silica fume, metakaolin and slag (Hay & Ostertag, 2021; Luo et al., 2022; Nguyen et al., 2021; Saha et al., 2018a; Tapas et al., 2021). Thus far, some publications have attempted the use of GP in GA-based cementitious materials. However, most of them focused on ASR mitigation effect while ignoring the mechanical and durability properties or used fixed fineness, colour or amounts of GW powder and aggregates (Liu et al., 2015; Hay et al., 2021; Sikora et al., 2017; Luo et al., 2022). It is to mention that the sorting of GW based on fixed categories can be costly and inefficient for recycling considering the large presence of this waste as mixed colour glasses (Imteaz et al., 2012; Liu et al., 2015) added different fineness of green soda-lime GPs to investigate the ASR of mortars prepared with up to 100% glass sand. According to their results, the ASR expansion risk of glass sand mortars can only be eliminated at GP content of 30% when its particle size is at the range of 15–100 μm . Idir et al., (2010) examined the use of 20% and 40% of mixed-colours soda-lime GP and 20% of GA by sand replacements to inhibit

the ASR swelling of mortars. The authors explained that the ability of GP to reduce ASR expansion is not solely related to its alkali trapping capacity by C–S–H and found ASR reductions of 50–90% and 25–70% for 40% and 20% GP, based on the mean size diameter of each powder and aggregates used. Very recently, Mahmood et al. (2022) tested the influence of 10% and 20% glass powder, as compared to fly ash, on the ASR expansion of mortars enclosing 20% and 40% of glass sand. They concluded that a 10% content of GP is enough to suppress the expansion risk at both 20% and 40% GA, which is equivalent to the effect of fly ash (Guo et al., 2018) characterized the ASR damage of GA-based mortars and evaluated the inclusion of 15% and 30% of GP and fly ash to decrease the related expansion. Although the expansion reduced by a minimum of 46.6% at 15% GP and fly ash replacement levels, only 30% GP content that resulted in percentages under the standardized expansion limit of 0.1%.

Very few studies considered the effect of GP on other hardened performances than ASR of glass sand mortars. Lu et al. (2017a, 2017b) used a content of 20% GP and explored the effect of its fineness on shrinkage, temperature resistance, acid attack and ASR swelling of glass sand mortars, as compared to fly ash. Although mixed colour glass waste was incorporated, only fixed contents of 20% GP and 100% glass sand were introduced into the mortar. They confirmed that, at 100% glass sand and 20% GP, a particle size of lower than 50 μm is important for GP to present equivalent performances than FA-based mortars. In another investigation by the authors (Lu et al. 2017a, 2017b), they studied the fresh properties of the same compositions with glass powder and glass aggregates and showed increased setting times and reduced flowability with the use of 20% GP, which was attributed to its low water absorption and different particle size and morphology than normal aggregates. Afshinnia and Rangaraju (2016) studied the impact of incorporating 20% of finely ground soda-lime GP (17 μm) by cement and sand replacements on the fresh and compressive, splitting and tensile strengths of concrete casted with up to 100% GA. According to these authors, the replacement of 20% of cement by high fineness GP increased the workability and reduced the mechanical strengths, whereas opposite trends were suggested when GP substituted aggregates in mortars. The above-mentioned work on the incorporation of GP in mortars containing GA focused more on the effect of GP size and type at 20% content on GA-based mortars, presenting opposite trend of results compared to Du and Tan (2014) and (2017) who reported that the substitution of cement by 30% GP in natural sand-based mortars exhibited the highest strength increase and consequently the lowest porosity.

In addition to the lack of consensus regarding the impact of GP on the properties of mortars containing GA aggregates, the technical literature does not report any attempts to optimize the composition of cementitious materials to include the maximum amount of GA and GP. Consequently, it is unclear to what extent GA and GP can be used conjointly without negatively affecting the mechanical and durability performances of mortars and/or concretes.

The aim of this study was to address the research gap regarding the optimized use of glass powder and glass sand in mortars.

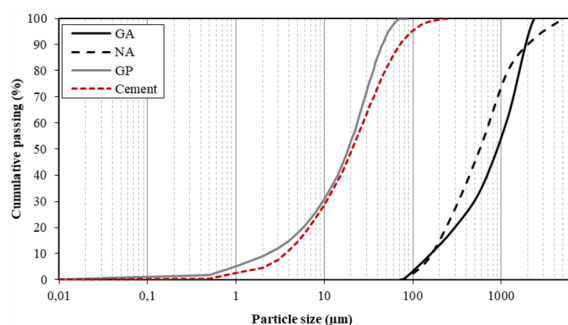
A detailed experimental program was undertaken to maximize the combined use of GA and GP in cementitious mortars while optimizing their mechanical and durability properties as compared to the control composition without any GW content. First, GA particles were treated with hydrofluoric acid (HF) to reach sufficient surface roughness (Park et al., 2017). Then they were included by natural sand replacement up to 100% and the best substitution level regarding the mechanical strengths was retained. Lastly, GP was introduced by cement replacement from 5 to 30% and the behaviour of each mixture was evaluated by assessing its compressive and flexural strengths, ASR effect and related microstructure, RCPT, sulphate and acid resistance.

2 Experimental Procedures

2.1 Materials

In this experimental work, Type I ordinary Portland cement (CEM I 42,5 N) was used in all the prepared mixtures, as conforming to the quality requirements of (ASTM C150 standard, 1997). The natural fine aggregates (NA) used in mortars were with a siliceous nature of average and maximum particle sizes of around 0.8 and 4.75 mm, respectively (ASTM C33-99a, 2010), and water absorption of 1.48%.

Glass waste (GW) was collected from real site dumping of crushed glasses, which included various colours (brown, green and transparent) of bottle, vessel and window glasses. This GW was washed to remove any contaminant and/or attached minerals. Then, it was crushed and used to prepare fine glass aggregates (GA) to pass completely in sieve 2.36 mm (Ling & Poon, 2011), and to be with close particle size distribution as NA. Extra milling process of 4 h was applied on crushed materials to obtain glass powder (GP) with finer particle sizes ($d_{(90)}$: 45 μm). The specific surface area of the resulted GP, was 3970 cm^2/g , as determined by the Blaine method. The particle size analysis of NA, GA, cement and GP is provided in Fig. 1 and the chemical compositions of cement, NA and GW are presented in Table 1.



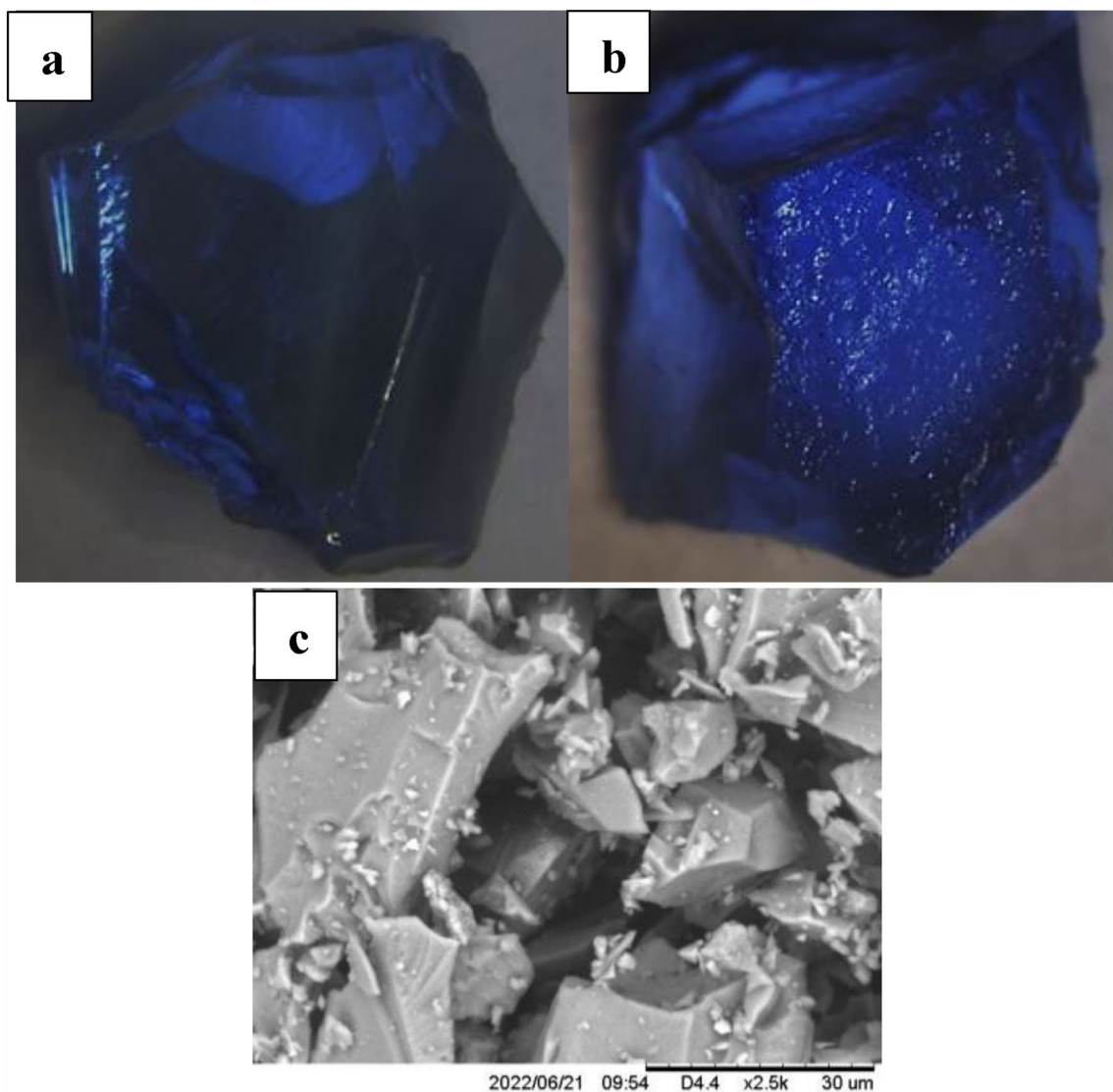


Fig. 2 Microscope and SEM images of **a** GA before treatment, **b** GA after treatment and **c** glass powder

incorporated in the control GA0. Different investigations in the literature have reported that it possible to increase the GA replacements to over 50% without significantly changing the strength of natural sand-mortars (Pena-cho et al., 2022; Sikora et al., 2017; Serati et al., 2021). According to these authors, the possible pozzolanic effect of smaller particles GA, which was confirmed even for GA particles of higher than 1 mm (Idir et al., 2011), can partially/completely compensate the negative influence of the coarse GA particles as compared to the inert counterparts of natural aggregates. In addition, the high alkalinity of GA likely depressed the solubility of Ca^{2+} ions and helped on the continuous reaction of cement particles and related strength development at different

curing ages (Siad, 2017). However, the optimized results presented in Fig. 3 also prove the efficiency of the treatment method by HF, which likely created enough GA surface roughness to enhance the bond with the surrounding cement matrix. Also, the improved GA surfaces and related increased physical and chemical interactions of aggregate/cement matrix interfaces, possibly caused greater distribution of stresses and related compressive strengths at early and advanced curing ages. It is to mention that the compressive strengths of GA100 were 12.5%, 6.7% and 3.2% lower than the control mixture at 7, 28 and 90 days, respectively, explaining reduced differences at increased curing times. This finding underscores the potential for achieving even higher outcomes from

Table 2 Compositions of the different mortars studied

Mix ID	Portland cement (g)	Glass powder (g)	Natural sand (g)	Glass sand (g)	Water (g)	Super-plasticizer (%)
GA0	500	–	1375	–	242.5	–
GA25	500	–	1031	344	242.5	0.25
GA50	500	–	687.5	687.5	242.5	0.3
GA75	500	–	344	1031	242.5	0.5
GA100	500	–	–	1375	242.5	0.7
GA75–GP5	475	25	344	1031	242.5	0.5
GA75–GP10	450	50	344	1031	242.5	0.5
GA75–GP15	425	75	344	1031	242.5	0.5
GA75–GP20	400	100	344	1031	242.5	0.5
GA75–GP25	375	125	344	1031	242.5	0.5
GA75–GP30	350	150	344	1031	242.5	0.5

Table 3 Greenhouse gas emissions of components of mortars

	Cement	GP	NA	Water	GA	SP
GHGs (kg CO ₂ /kg)	0.82	0.338	0.024	0.0013	0.008	0.6

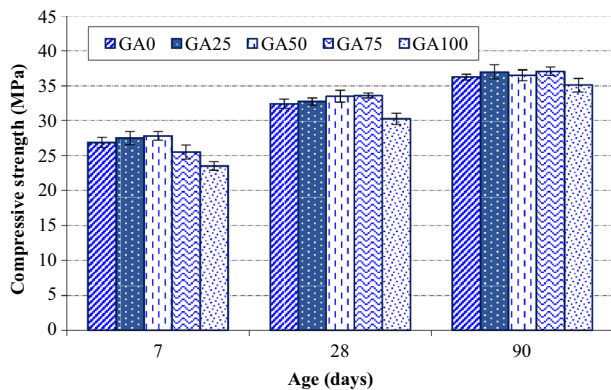


Fig. 3 Evolution of the compressive strength of GA mortars as a function of the age of the specimens

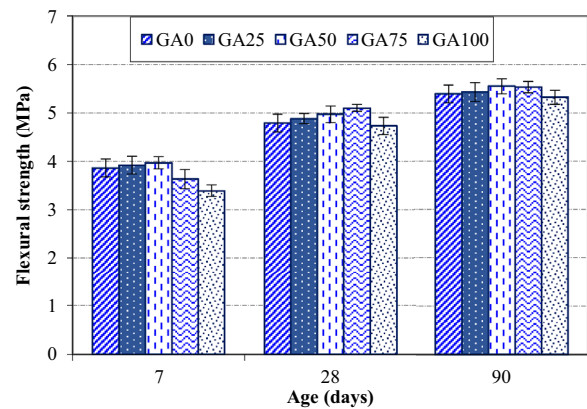


Fig. 4 Evolution of the flexural strength of GA mortars as a function of the age of the specimens

the pozzolanic activity of reduced GA particles when extending the curing duration, though this was not possible in this study considering the goal of determining the optimal GA content for the subsequent phases of the research.

The flexural strengths of various mortars shown in Fig. 4 followed the same trend as the compressive strengths up to 90 days, where GA75 generated the optimum mechanical strength development compared to the control mortar GA0. Nevertheless, the 7- and 28-day results presented negligible incidents of GA contents up to 75%, with a slight reduction of 7.5% for 100% GA

compared to the control GA0 compositions. Thus, a GA amount of 75% was decided to be used as the optimum in the next phase of research about glass powder, in accordance to the compressive and flexural strength results of GA-mortars. The rates and mixes of the GA75–GP 75% glass aggregate mortars to be tested in the next phase are also shown in Table 2.

2.3 Testing Methods

- Mechanical strengths: flexural, compressive strengths and ultrasonic pulse velocity (UPV) were

measured according to (ASTMC-348 standard, 2002; (ASTM C349-08, 2014) and (ASTM C 597-02, 2016), using specimen's dimensions of $(4 \times 4 \times 16)$ cm³ and $(4 \times 4 \times 4)$ cm³, respectively. Both mechanical strengths were measured at different curing ages of 7, 28 and 90 days. Three specimens were tested for flexural strengths and UPV, whereas the average value of 6 cubs was considered for compressive strengths.

- The properties of the interfacial transition zone (ITZ) of NA/binder and GA/binder were observed after 28 days using scanning electron microscope (SEM) and energy dispersive spectroscopy (EDS).
- Alkali-silica reaction: The influence of GP on the alkali-silica reaction (ASR) of mortars prepared with optimum GA content was investigated at various GP dosages from 5 to 30%. For this reason, mortar bars of $2.5 \times 2.5 \times 28.5$ cm³ were prepared, cured and tested according to (ASTM C1260 standard, 2007). After demoulding, the mortar bars were placed in hot water at a temperature of 80 ± 2 °C for 24 h. The reference length measurements were then taken before immersing the mortar bars in a 1N NaOH solution at a temperature of 80 ± 2 °C. Subsequent changes in length were measured after 3, 6, 9, 12 and 14 days of ASR test using a digital comparator with a precision of 0.001 mm. Each displayed result of length change was the average value of three tested specimens.
- The water permeability of mortars was estimated by their ability to be penetrated by water under a pressure gradient. Using a 3-cell device, measurements were made on cylindrical specimens of 100 mm diameter and 50 mm height, at the age of 90 days. The mortar specimens were covered laterally with a double layer of resin 24 h before the start of the test in order to avoid lateral leaks. Using a three-cell permeameter, the mortar discs were placed on a device under permanent water flow at a pressure of 0.3 MPa for 6 h (Kameche et al., 2014), the cumulative amount of water flowing through the mortar specimens as a function of time was measured every hour by decreasing the level in the manometer tube of the device. The coefficient of permeability was calculated by applying Darcy's law:

$$K_l = \frac{Q_l}{A \cdot i}, \quad (1)$$

where Q : volume of water per unit time (flow velocity). A : section crossed by water. K_l : permeability coefficient. i : hydraulic gradient across the specimen (m/m).

- Rapid chloride permeability test (RCPT): the test of resistance to chloride ions was done according to (ASTM C, 1202, 2012). Cylindrical specimens of 100 mm in diameter and 50 mm in height prepared for each mixture are shown in Table 3. The outer perimeter of the specimen was covered with epoxy resin to ensure a good seal. After curing, the specimens were placed in a desiccator to evacuate the air existing in the mortar using a vacuum pump for 3 h. Then the specimens were stored in water for 18 ± 2 h. One side of the specimens was exposed to a 3% NaCl solution, and the second side was exposed to 0.3N NaOH solution. The current between the electrodes was measured every 30 min for 6 h. The total charge passed through the specimens was calculated using the following equation:

$$Q = 900(I_0 + I_{360} + 2(I_{30} + I_{60} + I_{90} + \dots + I_{330})). \quad (2)$$

- The thermal conductivity (W/m.K) of mortars was measured using the thermal needle probe method according to (ASTM D5334, 2017), on 90-day-old cylindrical specimens of 100 mm diameter and 5 mm height. Thermal conductivity was determined by the KD2-PRO analyser using SH-1. The SH-1 contains two needles (1.27 mm diameter and 30 length) capable of measuring the thermal conductivity in the range of 0.2 W/m.K to 2 W/m.K. The measurements were repeated five times for each side of the specimen (Bostanci et al., 2020), the arithmetic averages of these measurements were reported as K -values.
- Resistance to sulphate attack: Penetration of $MgSO_4$ through the pores leads to the formation of magnesium silicate hydrate (M-S-H), and displaced calcium precipitates, mainly in the form of gypsum and causing ettringite. Three $(4 \times 4 \times 16)$ cm³ specimens of each mixture were placed in a 5% $MgSO_4$ solution tray following (ASTM C1012-04, 2004). The mass change for each sample was measured weekly after 12 weeks. The mass loss in % was calculated relative to the initial mass.
- Resistance to sulphuric acid: External chemical attacks are mainly due to acids, bases and saline solutions which dissolve the lime in cement and form new compounds, leading to the swelling and bursting of concrete structures, which can jeopardize their stability. According to Zivica and Bajza (2001), special precautions must be taken when working in submerged areas. To test the behaviour of new mortars in the face of this type of attack. Three $4 \times 4 \times 16$

cm³ specimens from each mixture were placed in a 5% H₂SO₄ solution in accordance with (ASTM C267, 2012). The average weight value of each sample was measured after 12 weeks while refreshing the solution after every measurement. The initial mass before immersion was utilized as a reference for different mass losses.

- To determine the environmental impact of GA and GP modified mortar samples, cradle-to-gate greenhouse gas (GHGs) emissions were measured for each material included in the mortar using the following equation (Ho and Huynh, 2022; Ameri et al., 2020):

$$\sum_{i=1}^n h_i \times m_i, \tag{3}$$

where h_i represents the CO₂ emission for each 1 kg for each material. m_i represents the mass of material in each 1 m³ of mortar.

In this study, HF acid are considered as a residual waste (Kusumawardaniet al., 2023; Toublanc, 2010), Consequently, the influence of HF acid and material transport on greenhouse gas emissions is neglected. GA and GP are produced from waste glass, which requires additional grinding to obtain smaller, finer aggregates.

Grinding GA requires electricity energy estimated at 0.0309 kW h in order to obtain recycled aggregate used as a building material (Crawford et al., 2019), while obtaining GP smaller than 100 μm has been estimated at 0.25 kW h (Pan et al., 2017). Greenhouse gas emissions per unit mass (1 kg) used in the calculations related to mortars were taken from the greenhouse gas emissions database of each material included: cement–GP (Pan et al., 2017), GA–NA–water (Crawford et al., 2019) and SP (Yu et al., 2017), as shown in Table 3.

3 Results and Discussion

3.1 Effect of GP Contents on Optimized GA-Mortar Strengths and Microstructure

3.1.1 Mechanical Strengths

Fig. 5 shows the effect of incorporating glass powder at 5–30% replacement levels with cement on the compressive strengths of GA75 mortars. As seen in this figure, the change of compressive strength with the increased inclusion of GP was based on the curing age of mortars. At 7 days, the results improved relatively at higher GP contents up to 10%, and after slightly reduced from 15 to 30% contents, with a maximum decrement of around 11% at GP amount of 30%. The small enhancement in the compressive strength at 5% and 10% GP amounts may explain a possible filling effect of the high fineness GP particles, which likely helped increasing the matrix packing density

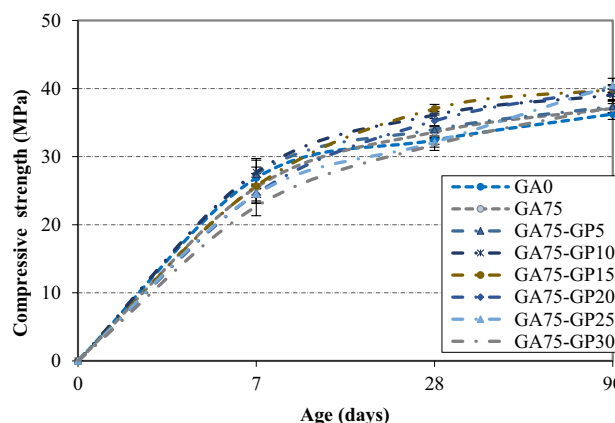


Fig. 5 Influence of glass powder on the compressive strength of GA mortars at different ages

to the benefit of the mechanical strengths (Aliabdo et al., 2016). This increase of strength from young age may be due also to the chemical reaction of SiO₂ reacts with the alkalis in the cement and GP to form a cementitious product that contributes to the development of mechanical strength (Vandhiyan et al., 2013). In addition, parts of GP possibly acted as nucleation sites for the additional formation of reaction products, resulting in improved hydration at early curing age of 7 days (Pan et al., 2017). Also, at 28 days, the strengths of GA-mortars increased when adding GP in the range of 5% to 20%, and reduced at 25% and 30%, while the optimum substitution level of GP was 25% at 90 days. The highest strength increments achieved at 28 and 90 days were 10.1% and 9.2% for GA75–GP15 and GA75–GP25 mortars compared to the reference GA75 composition. This larger amount of GP that can be added in GA75, while causing higher strengths at 90 days, can be related to the enhanced precipitation of C–S–H gel from the GP pozzolanic reaction, shown to develop and increase at advanced curing ages (Elaqra & Rustom, 2018b). This is also supported by the significant improvement of the mechanical strengths between the ages of 28 and 90 days for GA75GP20 (14.9%), GA75GP25 (26%) and GP75–GP30 (17.4%) mortars as compared to that of GA75 (10.3%). However, the over dosage of GP in GP75–GP30 mortar caused a slight decrement in the compressive strengths as compared to the optimum of 25% GP at 90 days, likely due to the reduced CH content with increased replacement of cement by GP, which was shown to slowdown the development of hydration and pozzolanic products (Shoaei et al., 2020).

The flexural strengths results displayed in Fig. 6 at different ages were generally in line with those of the compressive strengths, confirming the possibility of

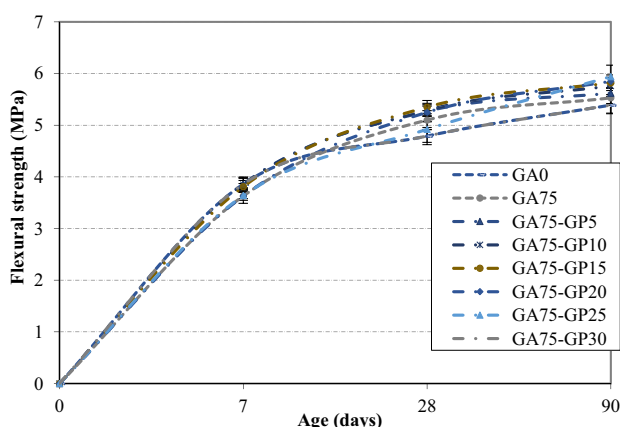


Fig. 6 Influence of glass powder on the flexural strength of GA mortars at different ages

incorporating up to 25% of GP in GA75 mortars while achieving optimized mechanical strengths at 90 days. This also indicates greater GA-to-paste ITZ properties with the enhanced use of GP, possibly because the developed reaction products from the pozzolanic reaction of GP particles, shown with a C–S–H system close to C–(N,K)–S–H with low Ca/Si (Pan et al., 2017; Elaqla and Rustom, 2018a, 2018b).

3.1.2 Microstructure

Aggregates/binder bonding properties in mortars are important for the transfer of stress in the matrix (Afshinnia & Rangaraju, 2015), thus highly affecting the resulted mechanical performance. SEM/EDS was preformed to assess the microstructural change and the quality of the bond between the treated GA and the surrounding binder in GA75 and GA75GP25 compositions as compared to the NA/binder in the control GA0. The SEM figures and related EDS data are provided in Fig. 7. The SEM images in Fig. 7b, c approve the roughened GA surfaces from the applied chemical treatment, which was intended to help improving their adhesion with the cement paste (Kusumawardani et al., 2023). High mechanical interlocking can be noticed between the treated GA and the surrounding paste, with no clear differences between the analysed NA-to-binder and GA-to-binder bonding properties in GA0, GA75 and GA75GP25 mortars. However, GA75GP25 showed a denser microstructure and more compact matrix around GA aggregates as compared to GA0 and GA75 compositions, in line with the previous explanation about the contribution of GP to the increased C–S–H development. The EDS results also support this explanation, since GA0, GA75 and GA75GP25 samples presented, respectively, reduced Ca/Si ratios of 2.87, 2.69 and 1.91 in relation to the higher

binding of silica at increased GA and GP contents. This indicates an enhanced matrix stiffness, in agreement with the increased mechanical strengths of mortars containing waste glass powder (Afshinnia & Rangaraju, 2015; Kong et al., 2016). In addition, GA75GP25 has the highest Na concentration of 2.8% as compared to GA0 and GA75 samples. According to Rashidian-Dezfouli and Rangaraju (2017), when silica increased compared to calcium (low Ca/Si ratios), the larger C–S–H density is anticipated to be close to C–(N, K)–S–H with higher alkalis in its structure, which can also help in reducing the risk of ASR damage in cementitious materials (Idir et al., 2010). Due to the lower Ca/Si ratio, the secondary charge of C–S–H became negative, favouring the absorption of cations in particular alkalis, leading to higher Na/Si ratios than primary C–S–H (Saccani et al., 2017). The production of these hydrates was similar when cementitious materials rich in reactive silica such as fly ash, blast furnace slag and fumed silica were added (Shayan, 2006; Taylor et al., 2007; Wang, 2009).

3.2 Effect of GP Contents on Optimized GA-Mortar UPV

Ultrasonic pulse velocity (UPV) was measured in order to investigate the evolution of porosity which can be influenced by the possible interlocking at the paste–aggregate interface (ITZ), as well as the evolution of the microstructure densification (the porous structure), especially after the inclusion of glass powder with high dosages.

The UPVs for all mixes at 7, 28, and 90 days curing age are shown in Fig. 8. A high UPV value in the mortars, indicate a dense structure which reflects the good performance of the mechanical strength. From Fig. 7, the UPV values of all (GA+GP)-based compositions increased with age, describing a strength development similar to that of the control with GW content. In addition, the UPV values for the (GA+GP)-specimens increased with GP rate up to 25% at 90 days, which support the previous discussion in the mechanical results. The increase in UPV after 90 days of age is related to the densification of the mortars after the formation of C–S–H by active silica in the GP. The reduction in UPV values in GA75–GP30 mortar is possibly explained to the reduced development of reaction products caused by the overdosing of glass which may have caused less compaction in the cementitious matrix of GA75–GP30 mortar than GA75–GP25. This is in line with the findings of Adaway and Wang (2015), who explained that at high replacement of cement per GP, the reduced amount of available CH from the diluted cement influenced negatively the developed C–S–H at different ages.

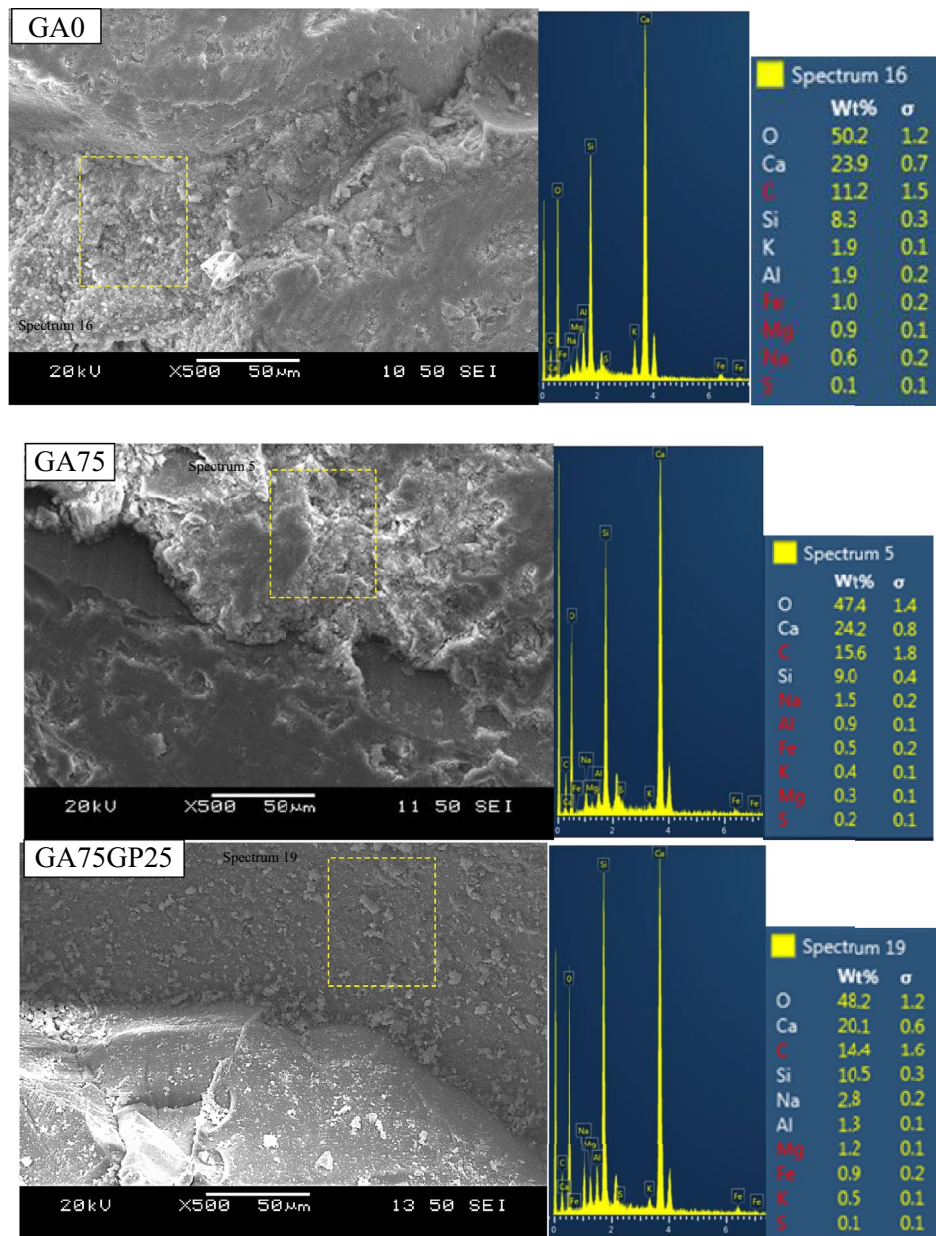


Fig. 7 SEM micrographs and EDS data of interfacial transition zones

3.3 Effect of GP Contents on ASR Expansions of Optimized GA-Mortar

The ASR expansion of GA75-mortars containing different amounts of GP as a partial replacement of cement is presented in Fig. 9. The curves of this figure showed increased expansion rates with advanced immersion time for all tested mortars immersed in NaOH solution at 80 ± 2 °C. The GA75-mortar generated the highest increments that attained a percentage of 0.182% at 14 days of ASR testing. This exceeded by 82% the limit of 0.1% provided in ASTM C1260 standard and

by around 172% the expansion of the reference mortar GA0, indicating a high ASR risk related to the use of 75% GA by NA replacement in mortars. However, the increased inclusion of GP in GA75 mortars caused the ASR expansion to reduce to almost equivalent results than GA0 mortar at 25% and 30% GP contents (0.082% and 0.071% expansions, respectively, at 14 days). In addition, lower swelling rates than the limit of 0.1% was registered for GA75–GP20 mixture, with 20% GP content, though the deleterious ASR effect was still existing at 5% to 15% of GP in GA75 mortars. This reveals

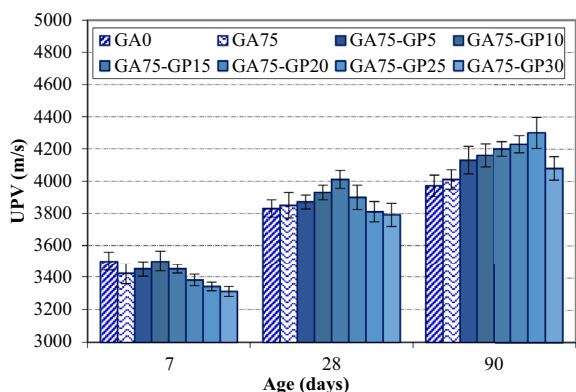


Fig. 8 Influence of glass powder on UPV of GA mortars

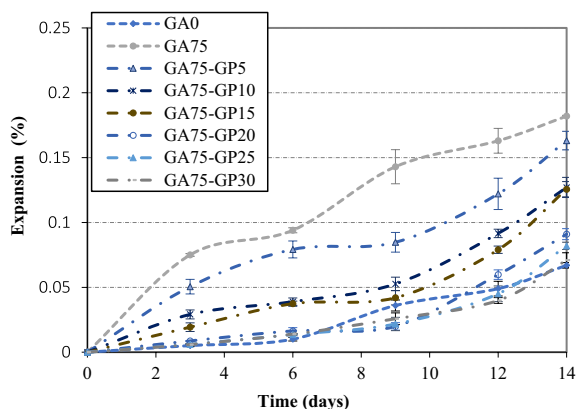


Fig. 9 Influence of glass powder on the expansion of mortars due to ASR

that, preventing the expansion risk in GA75 composition requires the incorporation of at least 20% GP, with higher reductions achieved at 25% and 30% GP amounts.

The siliceous nature of GP and the presence of high alkaline content in the network may have led to an accelerated pozzolanic reaction under the high temperature of 80 °C (Idir, 2009). Indeed, the positive influence of GP on highly reducing the expansion of the cementitious material was mainly shown to be related to its ability to consume the available amounts of calcium hydroxide (CH) (Afshinnia and Rangaraju et al., 2015; Omran et al., 2018; Konget et al., 2016; Siad et al., 2016). In addition, the consumption of most Ca^{+2} during the pozzolanic reaction of silica-rich GP, may also helped reduce an essential element that is shown necessary for the production of ASR gels, in addition to Na^+ , Ka^+ and OH^- (Lu et al. 2017a, 2017b). It is important to note that in the previous Fig. 7, a larger amount of sodium ($Na=2.8\%$) was present in GA75–GP25 sample, though this was accompanied with the lowest ASR expansion among all mortars. This

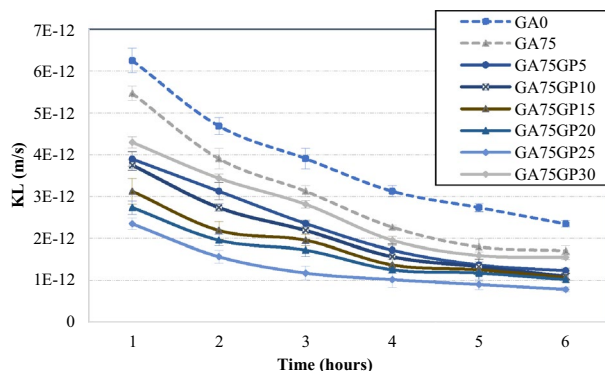


Fig. 10 Influence of glass powder on the water permeability of GA mortars

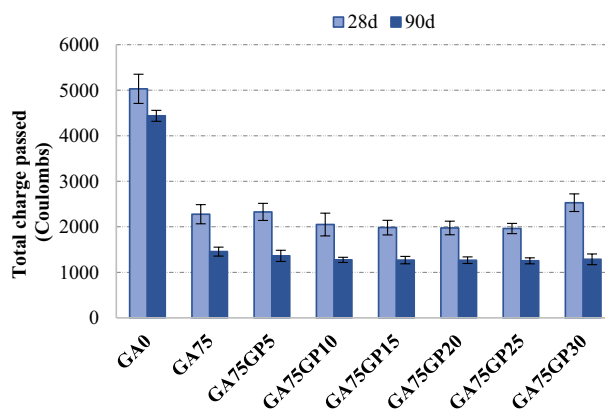


Fig. 11 Influence of glass powder on RCPT of GA mortars

supports the previous statement about the developed C–(N, K)–S–H and related increased retention of alkalis in GA75–GP25 sample, which caused the ASR risk to be suppressed.

3.4 Effect of GP Contents on Optimized GA-Mortar Water Permeability

The permeability coefficients as a function of time resulting from the mortar test are shown in Fig. 10. The curves express the influence of the combined use of GA and GP on the permeability of mortars, presenting water permeability values between $6.25E-12$ m/s and $7.81E-13$ m/s. From Fig. 10, the control GA0 composition displayed the highest water permeability compared to all GW-mixtures. Also, it was clearly noticeable that the amount of permeable water clearly reduced with the increased addition of GP in GA-mortars, except for 30% GP amount. Thus, the pozzolanic activity of GP at longer curing ages promoted also decreased capillary absorption ability (Rashidian et al., 2017), in line with its positive effect on enhancing the mechanical results at 90 days.

3.5 Effect of GP Contents on Optimized GA-Mortar RCPT

RCPT was measured on mortar cylinders at 28 and 90 days to evaluate the resistance of different mortars to chloride ion penetration. The results are shown in Fig. 11. The amount of chloride ions passed and penetrated into the mortars is less at 90 days of age. This is attributed to the densification of the structure of the material as a function of the curing age. The results also showed that the high amount of passing charge of the mortars was recorded by the GA0 at 5031 and 4438 coulombs at 28 days and 90 days. Control mortar GA0 showed the highest chloride penetration value compared to GA75 and all GA75+GP mortars. The large difference in permeability between NA- and GA-based cementitious mixtures was also noticed in the previous literature. According to Kou and Poon (2009), this can be attributed to the nature of glass particles which does not contain any internal porosity as compared to natural sand.

At 90 days the load passed through GA75 mortar presented a remarkable reduction of around 32% as compared to GA0. Therefore, the possible presence of reactive silica in the glass sand fines and the ability of treated GA to bond with the surrounding matrix may have increased the aptitude of the mortar to reduce the chloride permeability (Rashidian-Dezfouli & Rangaraju, 2017), especially at advanced age of 90 days. In addition, the mortars GA75GP5 to GA75GP25 performed better in reducing the Coulomb value than in the samples of GA75 at 28 days, but beyond GA75-GP25 the past load is more important, influenced by the dilution of cement and the associated structure of the materials which was less densified because the reduced formation of the C-S-H gel. Similar trend was also registered at the age of 90 days, where the load decreases according to the rate of GP up to 25%, where the values of the past load of the GA75-GPs are between 1455.2 to 1252.8 Coulombs. The clear advantage of using the glass waste in the mixture has influenced the penetration rate of chloride ions in both curing ages, where the amount of charge passing reduced depending on the amount of glass replacement in the mortars. According to ASTM C1202 (2012), the chloride ion permeability of mortars at 90 days is considered as low category (the passing charge is less than 2000 Coulombs), while GA0 is classified as high.

3.6 Effect of GP Contents on Thermal Conductivity of Optimized GA-Mortars

The thermal conductivity (k) value indicates the ability of mortars to transfer heat by conduction; a low conductivity value can explain a greater thermal insulation of mortars. The thermal conductivity results of (GA+GP)-samples are represented in Fig. 12. The thermal conductivity coefficient at 90 days was between 0.391 and 0.649

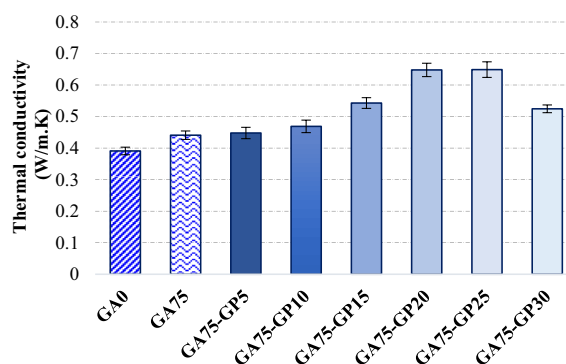


Fig. 12 Influence of glass powder on the thermal conductivity of GA mortars

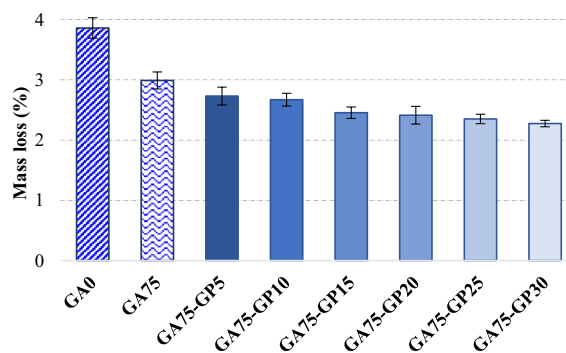


Fig. 13 Influence of glass powder on mass loss of mortars immersed in 5% MgSO₄

W/m.K for all mortars. The surface roughness of treated GA in GA75 and the use of pozzolanic GP in GA75GP mortars were discussed previously to develop a denser structure, which may have slightly increased the thermal conductivity of mixtures up to 25% GP content. For example, GA75, GA75GP25 and GA75GP30 compositions developed a thermal conductivity of 12.8%, 66% and 33% higher than that of GA0 at 90 days. This is in line with the finding of Bostanci (2020) who explained that the compacity variations of mortars represent the most impactful parameter on their thermal conductivity as compared to the material properties. Although the nature of waste glass, which contains a high amorphous silicon dioxide than silica sand, was intended to cause reduced thermal conductivity values than the control and GA75 mixture (Pan et al., 2017), the improved pore structure in (GA+GP) mortars seem to dominate the thermal conductivity results, leading to increased k at GP amounts of up to 25%.

3.7 Effect of Sulphate Resistance on Optimized GA-Mortars

The results of weight change of mortar specimens immersed in 5% $MgSO_4$ are shown in Fig. 13. So, it can be seen that the inclusion of glass waste in the mortar mixtures has improved their physical stability under magnesium sulphate, since the mass loss reduced in GA75 and all GP-based GA75 compositions as compared to that of the control GA0, regardless of the type and percentage of GW replacement. After 12 weeks, GA0, GA75 and GA75GP25 presented mass losses of 3.86%, 2.98% and 2.35% as compared to the sound state before magnesium sulphate.

GA75's good resistance than the control is likely due to its larger deposition of silicon–aluminium element, which led to a higher development of reaction products (Wang et al., 2016). The magnesium sulphate is shown in the literature to penetrate deep inside the specimens to cause the formation of Brucite ($Mg(OH)_2$) and gypsum, causing the degradation of cementitious sample (Skaropoulou et al., 2013). Thus, the stated increased compacity in GA75 and GA75-GP mortars likely helped in reducing the transport characteristics of the mortar and consequently the amount of deterioration. This is consistent with the explanations of Neville et al. (2004) who mentioned that the high strength cementitious composites contain lower porosity to accommodate the developed reaction formations. However, despite the stated decreased compacity due to the over dosage of GP in GA75GP30, the resistance to sulphate attack was almost similar, with a negligible improvement of 3.4%, as compared to GA75GP25. Therefore, in addition to CH, the larger GP rates may have also consumed a higher amount of tri-calcium aluminate hydrate in the mortars, leading to lower ettringite formation and related mass loss (Mansour et al., 2023).

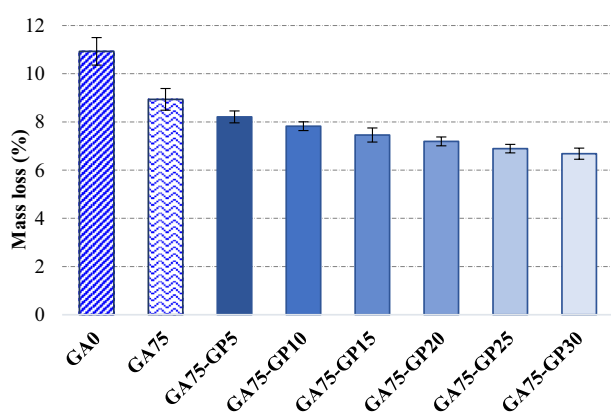


Fig. 14 Influence of glass powder on mass loss of mortars immersed in 5% H_2SO_4

3.8 Effect of GP on the Sulfuric Acid Resistance of GA-Mortars

The mass variation of mortars exposed to 5% H_2SO_4 is shown in Fig. 14. The mass loss started from the first two weeks of sulfuric acid immersion and continued with an increased trend at longer exposure time of all mortars. This was expected since the absorption of sulphuric acid at the surface of cementitious mortars was shown to form gypsum and secondary ettringite by reacting with the available CH and C–S–H. These harmful products are usually linked with volume change, spalling and degradation of cementitious materials (Konstantin et al., 2007). After 12 weeks of exposure to H_2SO_4 , the damage caused by the degradation of the top layer was noticeable for most mortars, especially for GA0 that presented a mass loss of 10.92% as compared to the initial mass before immersion. Although the use of 75% GA resulted in reduced total mass loss (8.93%) than GA0, lower mass losses were reached with increased GP integrations, reaching a percentage of 6.63% for GA75–GP30 specimens at 12 weeks of acid conditions. This can be related to the pozzolanicity of GP, which was explained earlier to help developing a denser and less porous microstructure, with the possible advantage of reducing the penetration of acid solution and related consumption of CH and C–S–H. In addition, according to Siad, (2017), the important effect of GP reaction-resulted C–S–H in binding the alkalis in its structure can change its configuration to be close to C–(N,K)–S–H, thus making the cement matrix more resistant to the deterioration by H_2SO_4 attack. This is also supported by the lower mass loss of GA75GP30, though this mixture presented previously higher open porosity and capillary absorption than all other GA75-GP mortars. Consequently, the higher risk of sulphuric acid penetration at 30% GP content was partially neutralized by the reduced available portlandite and generated C–(N,K)–S–H from the pozzolanic reaction of GP.

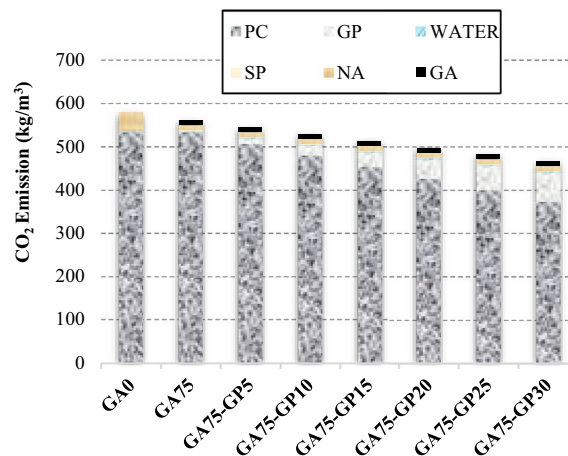


Fig. 15 GHGs emission of mortars

3.9 Environmental Impact of Mortars

A comparative ecological analysis of the combined impact of using GA and GP on GHG emissions is presented in Fig. 15, based on 1 m³ of mortar. The histograms show the total CO₂ emission of each mortar, released by the production or recycling of each component material. The influence of the constituent materials on the mortars was varied. The range of GHG emissions was, respectively: cement (between 373.70 and 533.90 kg CO₂/kg), GP (0–66.01 kg CO₂/kg), GA (0–10.74 kg CO₂/kg), SP (0–1.95 kg CO₂/kg) and NA (10.74–42.97 kg CO₂/kg), while water for all mortars represented an emission of only 2.60 kg CO₂/kg.

A comparative ecological analysis on the combined impact of using GA and GP on GHGs emissions is presented in Fig. 15 based on 1 m³ of mortar. The GA0 control mortar generated the highest CO₂ emission of all compositions at a value of 579.34 kg CO₂/kg. The decrease was somewhat noticeable when 75% GA, with a reduction of around 3.4% than the control GA0 with 100% NA. However, this clearly continued to decline as the amount of GP replacing PC increased to reach up to 19% and 16% reductions in GA75–GP25 compared to GA0 and GA75 compositions, respectively. Through an emission rate that varies between 80 and 95% of total GHGs in a mortar, the cement was the main contributor to greenhouse gas emissions in the prepared mortars; whereas the reuse of glass waste not only preserved the natural resources, but also significantly reduced CO₂ emissions in cementitious materials, in line with the previous studies about GA (Ho & Huynh, 2022) and GP (Pan et al., 2017).

4 Conclusions

This research investigated the possibility of combining high amounts of recycled glass waste aggregates and powder in the manufacturing of environmentally friendly mortars, with equivalent or greater mechanical, physical and durability properties than the control mortar with natural aggregates. The following conclusions can be drawn from this study:

1. It was possible to attain a replacement rate of 75% of NA with treated GA, while achieving improved performances in terms of compressive and flexural strengths as compared to the reference mortar.
2. The combined inclusion of glass powder and glass aggregates in GA75 mortar caused increased mechanical strengths, demonstrating a C–(N,K)–S–H development with reduced Ca/Si ratio at the optimum GP amount of 25%.
3. The UPV results supported the increased densification of GA75 mortars with the addition of GP up to

25%, describing a greater C–S–H formation especially at advanced age of 90 days.

4. Although the use of 75% GA in mortars highly exceeded their limit to ASR expansion, this was prevented at enhanced GP contents of more than 20% GP, with almost similar results than the control mortar at 25% and 30% GP contents. However, since the time of evaluation was limited to 14 days, considering the potential implications of glass in alkali silica reaction (ASR), long-term studies maybe needed to confirm the findings from this research study.
5. The ability of treated GA to bond with the surrounding matrix and the pozzolanic activity effect of GP in densifying the matrix were confirmed to cause GA + GP mixtures with decreased water and chloride permeabilities at longer curing age, though this also resulted in higher thermal conductivity values up to 25% GP content.
6. The inclusion of GP in GA75 mortar generated improved physical stability under magnesium sulphate, proven with the reduced mass loss at increased GP amounts and up to 12 weeks exposure to MgSO₄.
7. Like magnesium sulphate, the beneficial effect of C–(N,K)–S–H formation in GP-based GA75 mortars was confirmed to generate lower mass degradations and more resistant mortars to the deterioration by H₂SO₄ attack.
8. Although the environmental impact of the reference mortar was shown to decrease when using 75% GA, a remarkable reduction of around 19% was reached in the CO₂ emission when GP replacement by PC increased to 25%.

Acknowledgements

Not applicable.

Author contributions

SM: experiments, conceptualization, methodology, writing; ZK: supervision data analysis, validation; HS: supervision, writing, conceptualization, investigation, validation; ML: review and editing, project administration; MS: review and editing, supervision; YH: writing, review and editing, project administration. All authors read and approved the final manuscript.

Funding

Not applicable.

Availability of data and materials

All data generated or analysed during this study are included in this published article.

Declarations

Competing interests

There is no competing interest associated with the submission of this manuscript.

Received: 4 September 2023 Accepted: 7 February 2024
Published online: 01 May 2024

References

- Adaway, M., & Wang, Y. (2015). Recycled glass as a partial replacement for fine aggregate in structural concrete—effects on compressive strength. *Electronic Journal of Structural Engineering*, 14(1), 116–122. <https://doi.org/10.56748/EJSE.141951>
- Afshinnia, K., & Rangaraju, P. R. (2015). Influence of fineness of ground recycled glass on mitigation of alkali–silica reaction in mortars. *Construction and Building Materials*, 81, 257–267. <https://doi.org/10.1016/j.conbuildmat.2015.02.041>
- Afshinnia, K., & Rangaraju, P. R. (2016). Impact of combined use of ground glass powder and crushed glass aggregate on selected properties of Portland cement concrete. *Construction and Building Materials*, 117, 263–272. <https://doi.org/10.1016/j.conbuildmat.2016.04.072>
- Aliabdo, A. A., Abd Elmoaty, A. E. M., & Aboshama, A. Y. (2016). Utilization of waste glass powder in the production of cement and concrete. *Construction and Building Materials*, 124, 866–877. <https://doi.org/10.1016/j.conbuildmat.2016.08.016>
- Ameri, F., Shoaie, P., Reza Musaei, H., Alireza Zareei, S., & Cheah, C. B. (2020). Partial replacement of copper slag with treated crumb rubber aggregates in alkali-activated slag mortar. *Construction and Building Materials*, 256, 119468. <https://doi.org/10.1016/j.conbuildmat.2020.119468>
- American Society for Testing and Materials. (2010). ASTM C 33-99a : Standard Specification for Concrete Aggregates. *Annual Book of ASTM Standards*, i(C), 1–11.
- Anand, S. (2021). *What is driving the glass recycling market growth? Find the facts about glass recycling market.* <https://straitresearch.com/article/glass-recycling-market-growth>
- ASTM C1012-04. (2004). ASTM C1012-04 : Standard test method for length change of hydraulic-cement mortars exposed to a sulfate solution. *ASTM International*, 1–6.
- ASTM C1202. (2012). Standard test method for electrical indication of concrete's ability to resist chloride ion penetration. *American Society for Testing and Materials*, C, 1–8. <https://doi.org/10.1520/C1202-22.2>
- ASTM C349-08. (2014). Standard test method for compressive strength of hydraulic-cement mortars (using portions of prisms broken in flexure). *ASTM International*, 1–4. <https://doi.org/10.1520/C0349-18.2>
- ASTM C 597-02. (2016). Pulse velocity through concrete. *United States: American Society for Testing and Material*, 04(02), 3–6. <https://doi.org/10.1520/C0597-16.2>
- Bostanci, L. (2020). Effect of waste glass powder addition on properties of alkali-activated silica fume mortars. *Journal of Building Engineering*, 29, 101154. <https://doi.org/10.1016/j.jobe.2019.101154>
- Bueno, E. T., Paris, J. M., Clavier, K. A., Spreadbury, C., Ferraro, C. C., & Townsend, T. G. (2020). A review of ground waste glass as a supplementary cementitious material: A focus on alkali-silica reaction. *Journal of Cleaner Production*, 257, 120180. <https://doi.org/10.1016/j.jclepro.2020.120180>
- Cement, H., & Statements, B. (2002). *ASTM C-348 Standard Test Method for Flexural Strength of Hydraulic-Cement Mortars 1.04.*
- Chatterjee, S., Biswas, N., Datta, A., & Maiti, P. K. (2019). Periodicities in the roughness and biofilm growth on glass substrate with etching time: Hydrofluoric acid etchant. *PLoS ONE*, 14(3), e0214192. <https://doi.org/10.1371/JOURNAL.PONE.0214192>
- Chihaoui, R., Siad, H., Senhadji, Y., Mouli, M., Nefoussi, A. M., & Lachemi, M. (2022). Efficiency of natural pozzolan and natural perlite in controlling the alkali-silica reaction of cementitious materials. *Case Studies in Construction Materials*, 17, e01246. <https://doi.org/10.1016/j.cscm.2022.E01246>
- Crawford, R., Stephan, A., & Prideaux, F. (2019). *Environmental Performance in Construction (EPIc) Database: a database of embodied environmental flow coefficients*. 263. <http://minerva-access.unimelb.edu.au/handle/11343/233213>
- Du, H., & Tan, K. H. (2014). Waste glass powder as cement replacement in concrete. *Journal of Advanced Concrete Technology*, 12(11), 468–477. <https://doi.org/10.3151/jact.12.468>
- Du, H., & Tan, K. H. (2017). Properties of high volume glass powder concrete. *Cement and Concrete Composites*, 75, 22–29. <https://doi.org/10.1016/j.cemconcomp.2016.10.010>
- Elaqra, H., & Rustom, R. (2018a). Effect of using glass powder as cement replacement on rheological and mechanical properties of cement paste. *Construction and Building Materials*, 179, 326–335. <https://doi.org/10.1016/j.conbuildmat.2018.05.263>
- Elaqra, H., & Rustom, R. (2018b). Effect of using glass powder as cement replacement on rheological and mechanical properties of cement paste. *Construction and Building Materials*, 179, 326–335. <https://doi.org/10.1016/j.conbuildmat.2018.05.263>
- Guo, P., Meng, W., Nassif, H., Gou, H., & Bao, Y. (2020). New perspectives on recycling waste glass in manufacturing concrete for sustainable civil infrastructure. *Construction and Building Materials*, 257, 119579. <https://doi.org/10.1016/j.conbuildmat.2020.119579>
- Guo, S., Dai, Q., Sun, X., Xiao, X., Si, R., & Wang, J. (2018). Reduced alkali-silica reaction damage in recycled glass mortar samples with supplementary cementitious materials. *Journal of Cleaner Production*, 172, 3621–3633. <https://doi.org/10.1016/j.jclepro.2017.11.119>
- Higuchi, A. M. D., dos Santos Marques, M. G., Ribas, L. F., & de Vasconcelos, R. P. (2021). Use of glass powder residue as an eco-efficient supplementary cementitious material. *Construction and Building Materials*, 304, 124640. <https://doi.org/10.1016/j.conbuildmat.2021.124640>
- Ho, L. S., & Huynh, T. P. (2022). Recycled waste medical glass as a fine aggregate replacement in low environmental impact concrete: Effects on long-term strength and durability performance. *Journal of Cleaner Production*, 368, 133144. <https://doi.org/10.1016/j.jclepro.2022.133144>
- Idir, R. (2009). *Mécanisme d'action des fines et des granulats de verre sur la réaction alkali-silice et la réaction pouzzolanique* (Issue January).
- Idir, R., Cyr, M., & Tagnit-Hamou, A. (2010). Use of fine glass as ASR inhibitor in glass aggregate mortars. *Construction and Building Materials*, 24(7), 1309–1312. <https://doi.org/10.1016/j.conbuildmat.2009.12.030>
- Idir, R., Cyr, M., & Tagnit-Hamou, A. (2011). Pozzolanic properties of fine and coarse color-mixed glass cullet. *Cement and Concrete Composites*, 33(1), 19–29. <https://doi.org/10.1016/j.cemconcomp.2010.09.013>
- Imteaz, M. A., Ali, M. Y., & Arulrajah, A. (2012). Possible environmental impacts of recycled glass used as a pavement base material. *Waste Manag Res*, 30(9), 917–921. <https://doi.org/10.1177/0734242X12448512>
- Ismail, Z. Z., & AL-Hashmi, E. A. (2009). Recycling of waste glass as a partial replacement for fine aggregate in concrete. *Waste Management (New York, N.Y.)*, 29(2), 655–659. <https://doi.org/10.1016/j.wasman.2008.08.012>
- Kameche, Z. A., Ghomari, F., Choinska, M., & Khelidj, A. (2014). Assessment of liquid water and gas permeabilities of partially saturated ordinary concrete. *Construction and Building Materials*, 65, 551–565. <https://doi.org/10.1016/j.conbuildmat.2014.04.137>
- Kou, S. C., & Poon, C. S. (2009). Properties of self-compacting concrete prepared with recycled glass aggregate. *Cement and Concrete Composites*, 31(2), 107–113. <https://doi.org/10.1016/j.cemconcomp.2008.12.002>
- Kusumawardani, D. M., Wong, Y. D., Lwin, M. A., & Myo, T. Z. (2023). Evaluation of the feasibility of treated waste glass as aggregate in asphalt mixture. *Innovative Infrastructure Solutions*, 8(4), 1–9. <https://doi.org/10.1007/s41062-023-01095-9>
- Lee, G., Ling, T. C., Wong, Y. L., & Poon, C. S. (2011). Effects of crushed glass cullet sizes, casting methods and pozzolanic materials on ASR of concrete blocks. *Construction and Building Materials*, 25(5), 2611–2618. <https://doi.org/10.1016/j.conbuildmat.2010.12.008>
- Ling, T. C., & Poon, C. S. (2011). Utilization of recycled glass derived from cathode ray tube glass as fine aggregate in cement mortar. *Journal of Hazardous Materials*, 192(2), 451–456. <https://doi.org/10.1016/j.jhazmat.2011.05.019>
- Liu, S., Wang, S., Tang, W., Hu, N., & Wei, J. (2015). Inhibitory effect of waste glass powder on ASR expansion induced by waste glass aggregate. *Materials (Basel, Switzerland)*, 8(10), 6849–6862. <https://doi.org/10.3390/MA8105344>
- Lu, J., Duan, Z., & Poon, C. S. (2017). Fresh properties of cement pastes or mortars incorporating waste glass powder and cullet. *Construction and Building Materials*, 131, 793–799. <https://doi.org/10.1016/j.conbuildmat.2016.11.011>
- Lu, J. X., Zhan, B. J., Duan, Z. H., & Poon, C. S. (2017). Using glass powder to improve the durability of architectural mortar prepared with glass aggregates. *Materials and Design*, 135, 102–111. <https://doi.org/10.1016/j.matdes.2017.09.016>
- Mahmood, A. H., Afroz, S., Kashani, A., Kim, T., & Foster, S. J. (2022). The efficiency of recycled glass powder in mitigating the alkali-silica reaction induced by recycled glass aggregate in cementitious mortars. *Materials*

- and Structures/materiaux Et Constructions, 55(6), 156. <https://doi.org/10.1617/S11527-022-01989-7>
- Mansour, M. A., Ismail, M. H. B., Imran Latif, Q. B. A., Alshalif, A. F., Milad, A., & Bargi, W. A. (2023). A systematic review of the concrete durability incorporating recycled glass. *Sustainability (switzerland)*, 15(4), 3568. <https://doi.org/10.3390/SU15043568/S1>
- Manzoor, A., Yashpal, E., & Sharma, L. (2022). *Materials Today: Proceedings Comparison of partially replaced concrete by waste glass with control concrete*.
- Nahi, S., Leklou, N., Khelidj, A., Oudjit, M. N., & Zenati, A. (2020). Properties of cement pastes and mortars containing recycled green glass powder. *Construction and Building Materials*, 262, 120875. <https://doi.org/10.1016/j.conbuildmat.2020.120875>
- Omoding, N., Cunningham, L. S., & Lane-Serff, G. F. (2021). Effect of using recycled waste glass coarse aggregates on the hydrodynamic abrasion resistance of concrete. *Construction and Building Materials*, 268, 121177. <https://doi.org/10.1016/j.conbuildmat.2020.121177>
- Omrán, A., Soliman, N., Zidol, A., & Tagnit-Hamou, A. (2018). Performance of ground-glass pozzolan as a cementitious material—a review. *Advances in Civil Engineering Materials*, 7(1), 237–270. <https://doi.org/10.1520/ACEM20170125>
- Pan, Z., Tao, Z., Murphy, T., & Wuhler, R. (2017). High temperature performance of mortars containing fine glass powders. *Journal of Cleaner Production*, 162, 16–26. <https://doi.org/10.1016/j.jclepro.2017.06.003>
- Park, H., Cho, J. H., Jung, J. H., Duy, P. P., Tuan Le, A. H., & Yi, J. (2017). A review of wet chemical etching of glasses in hydrofluoric acid based solution for thin film silicon solar cell application. *Current Photovoltaic Research*, 5(3), 75–82.
- Penacho, P., de Brito, J., & Veiga, M. R. (2014). Physico-mechanical and performance characterization of mortars incorporating fine glass waste aggregate. *Cement and Concrete Composites*, 50, 47–59.
- Rajabipour, F., Maraghechi, H., & Fischer, G. (2010). Investigating the alkali-silica reaction of recycled glass aggregates in concrete materials. *Journal of Materials in Civil Engineering*, 22(12), 1201–1208. [https://doi.org/10.1061/\(ASCE\)MT.1943-5533.0000126](https://doi.org/10.1061/(ASCE)MT.1943-5533.0000126)
- Rashidian-Dezfouli, H., & Rangaraju, P. R. (2017). Role of ground glass fiber as a pozzolan in Portland cement concrete. *Transportation Research Record*, 2629(1), 33–41. <https://doi.org/10.3141/2629-06>
- Rivera, J. F., Cuarán-Cuarán, Z. I., Vanegas-Bonilla, N., & de Gutiérrez, R. M. (2018). Novel use of waste glass powder: Production of geopolymeric tiles. *Advanced Powder Technology*, 29(12), 3448–3454. <https://doi.org/10.1016/j.apt.2018.09.023>
- Romero, D., James, J., Mora, R., & Hays, C. D. (2013). Study on the mechanical and environmental properties of concrete containing cathode ray tube glass aggregate. *Waste Management*, 33(7), 1659–1666. <https://doi.org/10.1016/j.wasman.2013.03.018>
- Saccani, A., Bignozzi, M. C., Barbieri, L., Lancellotti, I., & Bursi, E. (2017). Effect of the chemical composition of different types of recycled glass used as aggregates on the ASR performance of cement mortars. *Construction and Building Materials*, 154, 804–809. <https://doi.org/10.1016/j.conbuildmat.2017.08.011>
- Serati, M., Jakson, N., Asche, H., Basireddy, S., & Malgotra, G. (2022). Sustainable shotcrete production with waste glass aggregates. *SN Applied Sciences*, 4, 82. <https://doi.org/10.1007/s42452-022-04967-4>
- Shayan, A. X. (2006). Performance of glass powder as a pozzolanic material in concrete: a field trial on concrete slabs. *Cement and Concrete Research*, 36(3), 457–468.
- Shoaei, P., Ameri, F., Reza Musaei, H., Ghasemi, T., & Cheah, C. B. (2020). Glass powder as a partial precursor in Portland cement and alkali-activated slag mortar: a comprehensive comparative study. *Construction and Building Materials*, 251, 118991. <https://doi.org/10.1016/j.conbuildmat.2020.118991>
- Siad, H. (2017). Potential for using recycled glass sand in engineered cementitious composites. *Magazine of Concrete Research*, 69(17), 905–918.
- Sikora, P., Horszczaruk, E., Skoczylas, K., & Rucinska, T. (2017). Thermal properties of cement mortars containing waste glass aggregate and Nanosilica. *Procedia Engineering*, 196(June), 159–166. <https://doi.org/10.1016/j.proeng.2017.07.186>
- Skaropoulou, A., Sotiriadis, K., Kakali, G., & Tsvilis, S. (2013). Use of mineral admixtures to improve the resistance of limestone cement concrete against thaumasite form of sulfate attack. *Cement and Concrete Composites, Complete*, 37, 267–275. <https://doi.org/10.1016/J.CEMCO.NCOMP.2013.01.007>
- Tahwia, A. M., Heniegal, A. M., Abdellatif, M., Tayeh, B. A., & Elrahman, M. A. (2022). Properties of ultra-high performance geopolymer concrete incorporating recycled waste glass. *Case Studies in Construction Materials*, 17, e01393. <https://doi.org/10.1016/j.cscm.2022.e01393>
- Tamanna, N., & Tuladhar, R. (2020). Sustainable use of recycled glass powder as cement replacement in concrete. *The Open Waste Management Journal*, 13, 1–13. <https://doi.org/10.2174/1874347102013010001>
- Taylor, R., Richardson, I. G., & Brydson, R. M. D. (2007). Nature of C-S-H in 20 year old neat ordinary Portland cement and 10% Portland cement-90% ground granulated blast furnace slag pastes. *Advances in Applied Ceramics*, 106(6), 294. <https://doi.org/10.1179/174367607X228106>
- Toublanc, C. (2010). *Amélioration du cycle trans-critique au CO2 par une compression refroidie : évaluations numérique et expérimentale To cite this version : HAL Id : tel-00465986 AMELIORATION DU CYCLE FRIGORIFIQUE TRANS-CRITIQUE AU CO 2 PAR UNE COMPRESSION REFRROIDIE : EVALUA.*
- United, T. H. E., & Of, S. (1997). By Authority Of. *ASTM C150: Standard Specification For Portland Cement*, 552(1), 203.
- Vandhiyan, R., Ramkumar, K., & Ramya, R. (2013). Experimental study on replacement of cement by glass powder. *International Journal of Engineering Research & Technology (IJERT)*, 2(5), 234.
- Wang, H. Y. (2009). A study of the effects of LCD glass sand on the properties of concrete. *Waste Management*, 29(1), 335–341. <https://doi.org/10.1016/J.WASMAN.2008.03.005>
- Wei, H., Zhou, A., Liu, T., Zou, D., & Jian, H. (2020). Dynamic and environmental performance of eco-friendly ultra-high performance concrete containing waste cathode ray tube glass as a substitution of river sand. *Resources, Conservation and Recycling*, 162, 105021. <https://doi.org/10.1016/j.resconrec.2020.105021>
- Yu, J., Lu, C., Leung, C. K. Y., & Li, G. (2017). Mechanical properties of green structural concrete with ultrahigh-volume fly ash. *Construction and Building Materials*, 147, 510–518. <https://doi.org/10.1016/j.conbuildmat.2017.04.188>
- Zhang, Y., Fan, Z., Sun, X., & Zhu, X. (2022). Utilization of surface-modified fly ash cenosphere waste as an internal curing material to intensify concrete performance. *Journal of Cleaner Production*, 358, 132042. <https://doi.org/10.1016/j.jclepro.2022.132042>

Publisher's Note

Springer Nature remains neutral with regard to jurisdictional claims in published maps and institutional affiliations.

Sarra Mezaouri Ph.D student, Department of Civil Engineering and Public Works, Ain-Temouchent University, Algeria.

Zine El-Abidine Kameche Senior Lecturer, Department of Civil Engineering and Public Works, Ain-Temouchent University, Algeria

Hocine Siad Research associate, Department of Civil Engineering, Toronto Metropolitan University, Toronto, Canada

Mohamed Lachemi Professor and President of Toronto Metropolitan University, Toronto, ON, Canada

Mustafa Sahmaran Professor, Department of Civil Engineering, Hacettepe University, Ankara, Turkey.

Youcef Houmadi Professor, Department of Civil Engineering, Tlemcen University, Algeria.